Identification of Secreted Proteins that Mediate Cell-Cell Interactions in an *In vitro* Model of the Lung Cancer Microenvironment

Li Zhong,[1] Jonathon Roybal,[1] Raghothama Chaerkady,[3,4] Wan Zhang,[1] Kuicheon Choi,[1] Cristina A. Alvarez,[1] Hai Tran,[1] Chad J. Creighton,[2] Shaoyu Yan,[1] Robert M. Strieter,[5] Akhilesh Pandey,[4] and Jonathan M. Kurie[1]

[1]Department of Thoracic/Head and Neck Medical Oncology, The University of Texas-M. D. Anderson Cancer Center; [2]Dan L. Duncan Cancer Center, Baylor College of Medicine, Houston, Texas; [3]Institute of Bioinformatics, International Technology Park, Bangalore, India; [4]McKusick-Nathans Institute for Genetic Medicine, Department of Biological Chemistry, The Johns Hopkins University School of Medicine, Baltimore, Maryland; and [5]Department of Medicine, University of Virginia, Charlottesville, Virginia

Abstract

Non–small cell lung cancer (NSCLC) cells with somatic mutations in *K-ras* recruit to the tumor a variety of cell types (hereafter collectively termed "stromal cells") that can promote or inhibit tumorigenesis by mechanisms that have not been fully elucidated. Here, we postulated that stromal cells in the tumor microenvironment alter the tumor cell secretome, including those proteins required for tumor growth and dissemination, and we developed an *in vitro* model to test this hypothesis. Coculturing a murine *K-ras* mutant lung adenocarcinoma cell line (LKR-13) with a murine lung stromal cell (macrophage, endothelial cell, or fibroblast) enhanced stromal cell migration, induced endothelial tube formation, increased LKR-13 cell proliferation, and regulated the secretion of proteins involved in angiogenesis, inflammation, cell proliferation, and epithelial-to-mesenchymal transition. Among these proteins, CXCL1 has been reported to promote NSCLC development, whereas interleukin-18 (IL-18) has an undefined role. Genetic and pharmacologic strategies to inhibit CXCL1 and IL-18 revealed that stromal cell migration, LKR-13 cell proliferation, and LKR-13 cell tumorigenicity required one or both of these proteins. We conclude that stromal cells enhanced LKR-13 cell tumorigenicity partly through their effects on the secretome of LKR-13 cells. Strategies to inhibit tumor/stromal cell interactions may be useful as therapeutic approaches in NSCLC patients. [Cancer Res 2008;68(17):7237–45]

Introduction

The tumor microenvironment is composed of structural (extracellular matrix), soluble (cytokines, proteases, and hormones, among others), and cellular components (tumor cells, fibroblasts, inflammatory cells, vascular and lymphatic endothelial cells, vascular smooth muscle cells, and pericytic cells, among others; ref. 1). Characterization of the inflammatory cells within tumors has revealed cells involved in both the adaptive and innate arms of the immune response. For example, dendritic cells in the microenvironment present tumor antigens to lymphocytes ($CD4^+$, $CD8^+$, and natural killer), promoting an antitumor response. A population of immature myeloid cells (called myeloid-derived suppressor cells) suppresses the antitumor cytotoxic T-cell response by promoting the development of $FOXP3^+$ $CD4^+$ T cells (Tregs) and inducing polarized differentiation of monocytes into tumor-associated macrophages (TAMs or M2 macrophages; ref. 1). TAMs, vascular endothelial cells, and fibroblasts within the tumor stroma secrete a number of growth factors and chemokines that promote tumorigenesis (1).

Chemokines, cytokines, and interleukins, which are expressed in leukocytes, endothelial cells, fibroblasts, tumor cells, and other cell types, regulate the trafficking of leukocytes and endothelial cells to sites of infection, inflammation, trauma, and malignancy (2, 3). Chemokines have been grouped into four subfamilies (CXC, CC, CX3C, and C, according to their structural cysteine motif found near the amino-terminus) and bind promiscuously to a family of G protein–coupled chemokine receptors (2). Consistent with their ability to respond to local environmental cues, proinflammatory chemokines and interleukins are present at high levels in the microenvironment of epithelial tumors. For example, non–small cell lung cancer (NSCLC) biopsy specimens have high intratumoral concentrations of CXCR2 ligands (CXCL1, CXCL5, and CXCL8) and type 2 cytokines [interleukin-4 (IL-4), IL-5, IL-10, and IL-13; refs. 4, 5]. However, the roles of these and other cytokines in the complex network of cell-cell interactions in the tumor microenvironment have not been fully elucidated.

Activating mutations in *K-ras* occur in ~10% of NSCLC specimens overall and 30% of the adenocarcinoma subtype (6). Several lines of evidence suggest that the *in vivo* transforming activity of oncogenic *K-ras* is mediated in part through epithelial cell nonautonomous mechanisms. In $Kras^{LA1}$ mice, lung adenocarcinomas that develop due to somatic activation of a latent oncogenic *K-ras* allele recruit macrophages, endothelial cells, neutrophils, and fibroblasts, a process driven in part by high expression of CXCR2 ligands (7, 8). Other mouse models that develop Ras-induced tumors are dependent upon expression of matrix metalloproteinases, vascular endothelial growth factor (VEGF), and CXCL8, which recruit inflammatory cells and endothelial cells to the tumor (9–12).

Here, we sought to further define the interactions between lung stromal cells and *K-ras* mutant lung cancer cells that promote lung tumorigenesis, an important question given that NSCLC patients might benefit from pharmaceutical strategies to target those interactions. We cocultured a lung adenocarcinoma cell line derived from $Kras^{LA1}$ mice (LKR-13) with cell lines derived from lung stroma and profiled the secreted proteins in the cocultures. We found that this *in vitro* model recapitulated features of the lung

Note: Supplementary data for this article are available at Cancer Research Online (http://cancerres.aacrjournals.org/).

L. Zhong and J. Roybal contributed equally to this work.

Requests for reprints: Jonathan M. Kurie, Unit 432, M. D. Anderson Cancer Center, 1515 Holcombe Boulevard, Houston, TX 77030. Phone: 713-792-6363; Fax: 713-792-1220; E-mail: jkurie@mdanderson.org.

©2008 American Association for Cancer Research.

doi:10.1158/0008-5472.CAN-08-1529

cancer microenvironment *in vivo* and identified novel mediators of cell-cell interactions that warrant further investigation of their roles in NSCLC development.

Materials and Methods

Cell lines. The derivation and culture conditions of the cell lines used in this study (LKR13, MEC, MHS, and MLg) have been described previously (7, 13–15). LKR-13 cells were a gift (Tyler Jacks, Massachusetts Institute of Technology), and the others were purchased from American Type Culture Collection.

Antibodies and recombinant peptides. We purchased recombinant murine peptides CXCL1, CXCL2, IL-18, and IL-18–binding protein (IL-18BP; R&D Systems); IL-18 ELISA kits (R&D Systems); IL-18 short hairpin RNA (shRNA) retroviral vectors (Open Biosystems); anti–total p38 antibodies, anti–phosphorylated p38 (Thr^{180}/Tyr^{182}) antibodies, anti–total extracellular signal-regulated kinase 1/2 (ERK1/2) antibodies, anti–phosphorylated ERK (Thr^{202}/Tyr^{204}) antibodies, and anti-p65 antibodies (Cell Signaling Technologies); RNeasy mini kit (Qiagen); PCR reagents (MMLV-RT, Rnasin, 5× MMLV buffer, Hexamer, bovine serum albumin, and deoxynucleotide triphosphate; Promega), PCR primers (Sigma Chemicals), and SYBR green PCR mix (Applied Biosystems) for quantitative PCR; and Transwell plates with 8-μm pores for migration assays (BD Biosciences). CXCR2 immune serum and normal goat immune serum were purified to isolate anti-CXCR2 neutralizing antibodies and control IgG, as described previously (7).

Migration assay. Cells (10^5) were plated in the bottom chambers of 24-well Transwell plates (BD Biosciences) in DMEM containing 10% serum and allowed to adhere for 4 to 6 h. After the membranes of the top chambers were coated with 0.1% gelatin, cells (5×10^4) were seeded into the top chambers, which were inserted into the bottom wells. The medium was then changed to serum-free DMEM. Each condition was evaluated in replicate (quadruplicate wells). For CXCR2 and IL-18 neutralization experiments, the cells in the upper chamber were pretreated for 1 h with anti-CXCR2 antibody (1:100) or IL-18BP (400 ng/mL) before placing the insert into the well. After incubation for 16 to 18 h, the conditioned medium was removed for use in later experiments, and the cells in the top chamber were fixed with 90% ethanol. Cells remaining on the seeded surface of the membrane were wiped off with a cotton swab, and the migrated cells on the undersurface of the membrane were stained with 0.1% crystal violet, washed with sterile double-distilled H_2O, and photographed. Five microscopic fields (4×) were counted per filter. Results were expressed as the mean ± SD of results from the replicate wells.

Tube formation assay. MECs (2×10^4) were plated onto 96-well plates coated with GFR-Matrigel (BD Biosciences) or the upper chambers of Transwell plates coated with GFR-Matrigel. Each condition was performed in replicate (quadruplicate wells). After coculture for 4 h, the numbers of enclosed tubes within the network were counted from five randomly chosen microscopic fields (4×). Results are expressed as the mean ± SD of results from the replicate wells.

Proliferation assay. We evaluated the ability of conditioned medium samples to induce cellular proliferation by using 3-(4,5 dimethylthiazol-2-thiazyl)-2,5-diphenyl-tetrazolium bromide (MTT, Sigma Chemical) assays. Briefly, LKR13 cells or stromal cells (3,000 per well) were plated in 96-well plates (four wells per condition). After 24 h, the cells were washed and treated with conditioned media samples in the presence or absence of different concentrations of recombinant peptides or antibodies. After 24 h, MTT solution (5 mg/mL) was added and the cells were incubated at 37°C for 3 h. The supernatant was aspirated, the cells were treated with DMSO (100 μL), and absorbance was measured at 570 nm. Results were expressed as the mean ± SD of results from replicate wells.

Cytokine quantification in conditioned medium samples. Mouse cytokine concentrations in conditioned medium samples were quantified by using Bio-Plex multiplex bead-based assays with mouse 23-plex and 9-plex kits (Bio-Rad Laboratories). This is a multiplexed, particle-based flow cytometric assay which uses anticytokine monoclonal antibodies linked to microspheres incorporating distinct proportions of two fluorescent dyes (16). For each cytokine calibration curve, eight standards were performed that ranged from 2.0 to 32,000 pg/mL. Data acquisition and analysis were completed by using the Bio-Plex 200 system with workstation (Bioplex Manager Software Version 5.0). Each condition was performed in replicate (triplicate conditioned medium samples) from which the means (±SD) were calculated. The assays were performed thrice, and results from one of the three assays are shown in Table 1.

***IL-18* shRNA transfection studies.** pSM2 retroviral scrambled shRNA control and murine IL-18 shRNAmir clones were purchased from Open Biosystems. The two IL-18–specific shRNAmir sequences used included (*a*) 5′-TGCTGTTGACAGTGAGCGACGCAGTAATACGGAATATAAATA-GTGAAGCCACAGATGTATTTATATTCCGTATTACTGCGGTGCCTACT-GCCTCGGA-3′ and (*b*) 5′-TGCT GTTGACAGTGAGCGCCCAAGTTCTC-TTCGTTGACAATAGTGAAGCCACAGATGTATTGTCAACGAAGAGAACT-TGGTTGCCTACTGCCTCGGA-3′. PT67 fibroblasts (Becton Dickson) were transfected with control or an IL-18–specific shRNAmir construct and selected for 21 d in 4 μg/mL puromycin to generate mass populations of retrovirus-producing cells. Supernatants from PT67 cells were concentrated using a 0.45-μm polyvinylidene difluoride filter. LKR-13 cells were exposed to retrovirus overnight. The media were then replaced with fresh media, and the transfectants were incubated overnight. To generate transient transfectants, this transfection process was repeated four times to increase the transfection efficiency and mass populations were used in the experiments. To generate stable transfectants, LKR13 cells were selected in puromycin (4.0 μg/mL) for 21 d and single cell subclones were isolated and expanded.

Colony formation assay. LKR-13 cells (2,500 cells per well in 0.5 mL of 0.8% soft agarose) were seeded into 12-well plates layered with 1.8% agar. Each condition was performed in replicates (triplicate wells). Cells were treated with conditioned medium samples for 14 d and fixed and stained with crystal violet/methanol (0.005% in 20% methanol). Visible colonies were counted using a microscope (4× magnification).

Quantitative PCR assay. RNA was isolated from cells (RNeasy mini kit), and 2 μg of each RNA sample were reverse-transcribed. PCR analysis was performed using the ABI 7500 Fast Real-Time PCR System (Applied Biosystems). The comparative threshold method was used using glyceraldehyde-3-phosphate dehydrogenase (GAPDH) as an endogenous reference housekeeping gene. Serial dilutions of a mixture of cDNA samples were used as the standard curve for each reaction. SYBR green I was used as the fluorophore. All experiments were performed in triplicate. The primer sequences were as follows: GAPDH forward 5-TGAAGCAGGCATCT-GAGGG-3, reverse 5-CGAAGGTGGAAGAG TGGGAG-3; CXCL1 forward 5′-GCACCCAAACCGA AGT CATA-3′, reverse 5′-TGGGGACACCTTTTAG-CATC-3′; CXCL2 forward 5′-AGCCT GGATCGTACCTGATG-3′, reverse 5′-TAACAAC ATCTGGGCAATGG-3′.

Western blot analysis. Lysates from cell lines were separated by SDS-PAGE and transferred onto a polyvinylidene fluoride nitrocellulose membrane (Bio-Rad Laboratories). Membranes were immunoblotted overnight at 4°C with primary antibodies in TBST containing 5% nonfat dry milk. Antibody binding was detected with an enhanced chemiluminescence kit according to the manufacturer's instructions (Amersham).

Sample preparation for quantitative proteomics. LKR13 cells were grown in the presence of $^{13}C_6$-arginine + $^{2}H_4$ lysine (medium) and $^{13}C_6^{15}N_4$-arginine + $^{13}C_6^{15}N_2$ lysine (heavy) labeled amino acids; MHS, MEC, MLg cells were grown in light (no label) and heavy amino acids (Cambridge Isotope Labs.). A detailed protocol for stable isotope labeling with amino acids in cell culture (SIL-AC) media preparation is described (17, 18) and is available online.[6] The cells were adapted to SIL-AC media by allowing five passages of cell culture, and completion of labeling was checked by performing in-gel digestion and mass spectrometry analysis using cells collected at the end of five passages. At the end of the fifth passage, an equal number of MEC, MHS, and MLg grown in heavy media were cocultured with three sets of LKR13 cells cultured in heavy media. For example, MHS/Heavy 5×10^4 cells/5 mL were cocultured with LKR13 cells (5×10^4 cells/5 mL) grown in

[6] http://www.silac.org

Table 1. Concentrations of chemokines and cytokines in conditioned media samples from monoculture and coculture based on multiplexed antibody bead assays

Mean (±SD)		Cells in culture (monoculture or coculture)						
		LKR13	MHS	MEC	MLg	MHS/LKR13	MEC/LKR13	MLg/LKR13
Chemokines (pg/mL)	MCP-1/CCL2	92.66 (9.05)	270.78 (41.5)	484.89 (6.07)	1296.18 (168.39)	916.16* (65.62)	416.55 (78.42)	341.84 (131.62)
	MIP-1a/CCL3	41.11 (1.68)	—	45.10 (3.10)	55.93 (5.77)	873.24* (197.48)	42.34 (2.57)	85.21 (4.49)
	MIP-1b/CCL4	2.90 (1.13)	2740.85 (282.56)	3.16 (0.43)	9.28 (2.60)	60.89 (7.20)	6.78 (1.29)	5.48 (3.14)
	RANTES/CCL5	—	12697.67 (4843.35)	115.13 (48.89)	28.93 (2.22)	22.05 (1.53)	—	—
	EOTAXIN/CCL11	349.34 (63.20)	366.16 (30.22)	347.76 (15.52)	662.20 (88.83)	372.50 (6.35)	247.02 (25.00)	337.33 (65.78)
	KC/CXCL1	205.33 (8.62)	—	143 (8.72)	40.86 (5.56)	5246.33* (149.22)	4070.33* (578.84)	1817.00* (166.58)
	MIP-2/CXCL2	2.22 (0.70)	13.72 (1.36)	—	—	969.54† (59.38)	26.95† (6.25)	22.92 (7.77)
	MIG/CXCL9	—	—	—	—	16.28 (2.50)	—	—
Growth Factors (pg/mL)	bFGF	—	—	—	24.68 (1.13)	10.00 (1.41)	9.00 (0.10)	4.00 (0.00)
	PDGFβ	—	—	—	—	—	—	—
	VEGF	849.65 (196.43)	—	46.27 (3.62)	504.55 (40.04)	1684.52* (466.62)	2101.63* (205.61)	2383.64† (534.12)
Interleukins (pg/mL)	IL-1a	—	—	—	5.42 (0.78)	—	—	—
	IL-1b	14.74 (1.61)	119.96 (11.30)	16.50 (2.29)	30.10 (1.06)	64.47 (3.97)	21.87 (2.45)	14.54 (6.48)
	IL-2	—	—	—	10.06 (0.82)	—	—	—
	IL-3	—	—	—	—	—	—	—
	IL-4	—	—	—	0.45 (0.11)	—	—	—
	IL-5	—	—	—	—	—	—	—
	IL-6	—	1.47 (0.28)	2.44 (0.14)	2.27 (0.86)	26.15* (2.21)	4.85 (0.97)	—
	IL-9	8.08 (3.39)	15.16 (2.97)	8.54 (2.82)	16.02 (5.97)	25.37 (3.07)	19.87 (2.43)	16.29 (2.19)
	IL-10	4.19 (1.23)	14.40 (1.98)	5.88 (0.67)	15.28 (1.84)	8.09 (0.26)	4.92 (0.46)	3.82 (1.02)
	IL-12 (p40)	—	—	—	—	—	—	—
	IL-12 (p70)	13.64 (1.07)	17.57 (2.60)	15.71 (3.10)	17.81 (1.70)	13.83 (2.09)	13.18 (0.13)	13.13 (2.53)
	IL-13	66.56 (9.07)	178.63 (24.91)	95.72 (4.87)	164.27 (13.24)	161.14 (3.83)	98.493 (9.66)	55.92 (34.05)
	IL-15	6.085 (1.11)	—	—		187.95* (88.15)	42.61* (5.99)	30.94 (15.24)
	IL-17	—	—	—	—	—	—	—
	IL-18	3.11 (0.53)	—	—	—	133.52* (70.01)	48.04* (10.58)	33.29* (7.55)
Other cytokines (pg/mL)	G-CSF	—	—	—	—	221.22* (54.75)	—	—
	GM-CSF	6.34 (0.23)	5.35 (0.24)	2.52 (0.38)	9.65 (0.01)	70.52* (5.19)	23.47† (6.06)	90.60† (21.98)
	IFNγ	3.37 (1.10)	4.31 (0.23)	3.28 (0.19)	8.67 (2.95)	3.40 (0.61)	3.07 (0.28)	6.26 (0.64)
	TNFα	5.84 (0.94)	5.8 (1.14)	5.76 (0.68)	23.30 (1.17)	79.59* (8.97)	9.46 (0.26)	8.25 (0.79)
	LIF	18.63 (4.07)	—	8.14 (2.29)	2.69 (0.75)	169.11* (59.55)	120.05* (5.04)	157.67* (65.09)

NOTE: The illustrated results are from one experiment and representative of results from three experiments. Values are the means of triplicate samples. (—) designates undetectable levels.

*$P < 0.01$.

†$P < 0.05$.

heavy media for 24 h. The two types of cells were separated by using a strainer mesh. Simultaneously, 5 mL of cell-free media were also collected from same number of MHS cells and LKR13 cells labeled with light and medium amino acids, respectively. These three supernatants (cell ratio, 1:1:2) were combined in the presence of protease inhibitor cocktail tablets (Roche Applied Science) and concentrated using Centriprep YM-3 (Millipore). The samples were then separated on one-dimensional SDS-PAGE (10%), and bands were visualized using colloidal Coomassie staining. The protein bands were excised, reduced, alkylated, and digested with trypsin as previously described (18). Supernatants from the in-gel digestion were collected by three consecutive extractions using 0.1% formic acid, 0.1% formic acid, 50% acetonitrile and acetonitrile and dried in vacufuge.

Liquid chromatography–mass spectrometry. Dried peptides were reconstituted in 10 μL 0.2% formic acid and analyzed using reversed phase liquid chromatography tandem mass spectrometry (LC-MS/MS). The liquid chromatography system used (Agilent 1100 series) is designed to deliver solvent at 1 μL/min flow for sample loading and cleaning on the precolumn and at 250 to 300 nL/min for peptide fractionation on the analytic column. Precolumn (ID-75 μm, 3 cm) was packed with 5 to 10 μm C18 ODS-A (YMC Co.), and the analytic column (ID-75 μm, 10 cm) was packed with 5 μm Yydac C18 resin (Nest Group). An emitter tip of 8 μmol/L (New Objective) was attached. The columns were equilibrated with 95% solvent A containing 0.4% formic acid (0.005% heptafluorobutyric acid, v/v) before applying peptide to the column. Peptides were separated using a linear gradient (90% of solvent A to 40% of solvent B, 90% acetonitrile, 0.1% formic acid, 0.005% heptafluorobutyric acid, v/v) for 30 min. The LC-MS/MS analysis was performed using a Micromass Q-ToF US-API mass spectrometer (Waters) in a data-dependent manner, choosing the three most abundant ions selected for MS/MS analysis and further excluded for 45 s.

Mass spectrometry data were acquired using Masslynx (Version 4.0). The following settings were used for automated data collection: ion mass window, 2.5 Da; intensity threshold for MS/MS to MS switch, 5 counts/s; MS to MS/MS switch, 20 counts/s; scan time for MS and MS/MS, 1 s each; number of scans per cycle, 3; and total cycle time, 10 s with an interscan delay of 0.1 s. Peak list files (pkl) from individual MS/MS scans were generated using Masslynx with the following variables: smooth window, 4.0; number of smooths, 2 (Savitzky Golay smooth mode). Using a perl script, pkl files from each LC-MS/MS experiment were combined to

generate a Mascot-readable file, which were searched using Mascot v2.2.0 (Matrixscience) against RefSeq 26 mouse database (dated 11/04/2007) containing 20,311 sequences. The following modifications were included, whereas searching the database carbamidomethylation of cysteine was set as a fixed modification and $^{13}C_6$-arginine, $^{13}C_6^{15}N_4$-arginine, $^{2}H_4$ lysine, $^{13}C_6^{15}N_2$ lysine, and oxidation of methionine were set as variable modifications. The mass tolerance was set at 0.2 atomic mass units for precursor and 0.5 atomic mass units for fragmented ions. Relative quantitation of SIL-AC–labeled peptides was performed using MSQuant downloaded from http://msquant.sourceforge.net (19). Mascot search results in .html format were parsed with the raw data file in MSQuant. Under quantitation modes, the masses of the medium and heavy arginine and lysine residues were added for MSquant to recognize the MS peaks from raw files for quantitation. The quantitation data were verified by manual inspection of the heavy and light peptides derived from MS and MS/MS spectra in MSQuant. Fold-changes were calculated for the SIL-AC MS clusters with at least one peak corresponding to >30 mascot score. The average protein ratio was calculated based on the individual ratios obtained for all peptides derived from a specific protein.

Mouse experiments. Before their initiation, all mouse studies were submitted to and approved by the Institutional Animal Care and Use Committee at the University of Texas-M.D. Anderson Cancer Center. Mice received standards of care and were euthanized according to the standards set forth by the IACUC. 129/SV mice (n = 4 per group) were injected s.c. in the right flank with 10^6 LKR-13 cells that had been stably transfected with *IL-18*–specific shRNA or scrambled control retroviral vectors. Mice were monitored daily for growth of tumor and sacrificed after 21 d. The tumors were removed, photographed, and formalin-fixed.

Results

Coculture model. A coculture model was created using LKR-13 cells and one of three immortalized murine lung stromal cell lines, including a fibroblast (MLg), an endothelial cell (MEC), and a macrophage (MHS). LKR-13 cells were chosen for this model because they potently chemoattract inflammatory cells and endothelial cells when injected s.c. into nude mice (7, 8). The cells were cultured in Transwell plates containing two chambers separated by a porous membrane that allowed bidirectional diffusion of secreted, soluble mediators. For endothelial tube formation assays, MECs were seeded onto a layer of growth factor-reduced Matrigel covering the porous membrane. Cells migrating across the porous membrane and MEC endothelial tubes were counted. Conditioned media samples were collected from these cocultures to measure cytokine concentrations and to examine their mitogenic effects on cells.

The migration of stromal cells in monocultures was sharply enhanced by coculturing them with either LKR-13 cells or each other (Fig. 1*A*). The stromal cells only weakly chemoattracted LKR-13 cells (Fig. 1*A*), which was not due to a defect in the ability of LKR-13 cells to migrate based on our finding that fetal bovine serum (10%) potently chemoattracted LKR-13 cells (data not shown). Cultured alone, MECs developed no tubes, but tubes formed when MECs were cocultured with any of the other cell types (Fig. 1*B*). Treatment with conditioned medium samples increased the proliferation of LKR-13 cells and MECs but not the other stromal cells (Fig. 1*C*). LKR-13 colony formation in soft agar was enhanced by treatment with conditioned medium samples from MECs (monoculture or coculture) and LKR-13/MLg cocultures (Fig. 1*D*). Collectively, these findings showed bidirectional interactions between LKR-13 cells and stromal cells through the secretion of soluble mediators.

Chemokine and cytokine regulation in cocultured cells. We assessed the mediators secreted by cells in monoculture and coculture by performing multiplexed cytokine assays on conditioned media samples. Of the 32 proteins examined, 27 were detectable at the limits of sensitivity of this assay (1 pg/mL; Table 1). The chemokines and cytokines that were most abundant (≥50 pg/mL) in the monocultures were CCL2, CCL3, CCL4, CCL5, CCL11, CXCL1, VEGF, IL-1β, and IL-13. Those that increased in the cocultures based on the criterion of at least a 2-fold increase in concentration relative to that of the monocultures were CCL2, CCL3, CXCL1, CXCL2, VEGF, IL-15, IL-18, granulocyte colony stimulating factor, granulocyte-monocyte colony stimulating factor, tumor necrosis factor-α (TNF-α), and leukemia inhibitory factor (LIF; Table 1). The majority of these were undetectable in monocultured cells, indicating that the cytokines expressed basally were distinct from those regulated by cell-cell interactions. Although LKR-13 cell densities increased by ~50% in coculture, this was far less than the increases in cytokine concentrations. For example, KC increased 9-fold to 20-fold in the cocultures and IL-18 increased 10-fold to 44-fold (Table 1), indicating that the changes in LKR-13 cell density cannot account for the changes in these cytokine concentrations.

Regulation of extracellular matrix proteins, cell adhesion molecules, and proteases in cocultures. To further assess the spectrum of biological processes in the cocultures and the secreted proteins that mediate these processes, SIL-AC assays were performed on conditioned media samples obtained from the three coculture experiments. The secreted proteins were profiled, and the relative abundance of each protein was compared in monoculture and cocultures. A total of 299 proteins were isolated and sequenced from the three experiments (83 in MHS/LKR-13, 82 in MEC/LKR-13, and 134 in MLg/LKR-13), 181 of which were found to be unique proteins (Supplementary Table S1). Examples of the MS/MS spectra obtained from the SIL-AC assays are illustrated in Supplementary Figs. S1 to S4. These proteins did not include any of the cytokines identified by the multiplexed antibody assays (Table 1) because the lower limit of sensitivity for SIL-AC is ~1 μg/mL, which exceeded the concentrations of cytokines identified by the multiplexed antibody assays (Table 1).

Based on the criterion of at least a 2-fold difference between monoculture and cocultures, the abundance of certain proteins changed in the cocultures (Supplementary Table S2). For example, in monoculture, LKR-13 cells secreted extracellular matrix and cell surface molecules involved in cell adhesion (tenascin XB, calsyntenin-1, E-cadherin, biglycan, and agrin), proteases that promote invasion (osteopontin and cathepsin H), a prosurvival molecule (clusterin), and proangiogenic molecules (CX3CL1, vascular cell adhesion molecule-1, and agrin), all of which decreased in the cocultures. The reduction in cell adhesion molecules, including E-cadherin (Supplementary Table S2), has been reported in cancer cells that have undergone epithelial-to-mesenchymal transition (EMT; ref. 20). Thus, a number of proteins with a broad range of biological functions in the extracellular matrix were regulated in the cocultures.

In addition to these extracellular matrix proteins, a number of intracellular proteins (i.e., transaminases, dehydrogenases, and RNA-binding proteins) were identified by the SIL-AC assays (Supplementary Table S1). This leakage of intracellular proteins into the media suggested that cell lysis had occurred. However, examination of the cocultures revealed no evidence of floating cells, and Western analysis of the adherent cells for caspase-3 cleavage revealed no detectable evidence of apoptosis (data not shown), suggesting that the level of cell death in the cocultures was minimal.

Role of CXCL1 and IL-18. CXCL1 was the most abundant chemokine detected in the cocultures (Table 1). CXCL1 RNA levels increased in cocultured LKR-13 cells but not in cocultured stromal cells (Supplementary Fig. S5*A*), indicating that LKR-13 cells were the primary source of CXCL1 in the cocultures. Similarly, lung tumors obtained from $Kras^{LA1}$ mice have high CXCL1 expression, and the growth of these tumors is dependent upon CXCR2, the primary receptor for CXCL1 (2). To assess whether the *in vitro* model was CXCR2-dependent, we treated the cocultures with an anti-CXCR2 neutralizing antibody (7). CXCR2 neutralization decreased the ability of LKR-13 cells to chemoattract stromal cells and attenuated LKR-13 cell colony formation in soft agar (Supplementary Fig. S5*B* and *C*), demonstrating that these features of the cocultures were CXCR2-dependent.

A cytokine that increased in all three cocultures was IL-18 (Table 1), a member of the IL-1 family that can either inhibit tumorigenesis by activating interferon-γ production in natural killer cells or promote it by enhancing VEGF secretion from tumor cells (21). Because VEGF and IL-18 levels were coordinately regulated in these cocultures (Table 1), we postulated that IL-18 promotes cell-cell interactions in this model. IL-18 was inhibited pharmacologically by treating the cultures with IL-18BP, which neutralizes IL-18 biological activity (22). Pretreatment with IL-18BP inhibited the ability of conditioned media samples from cocultures to enhance stromal cell migration and LKR-13 colony formation (Fig. 2*A* and *B*). Treatment of MECs with recombinant IL-18 induced tube formation (Fig. 2*C*), but the addition of IL-18BP did not abrogate tube formation induced by treatment with coculture

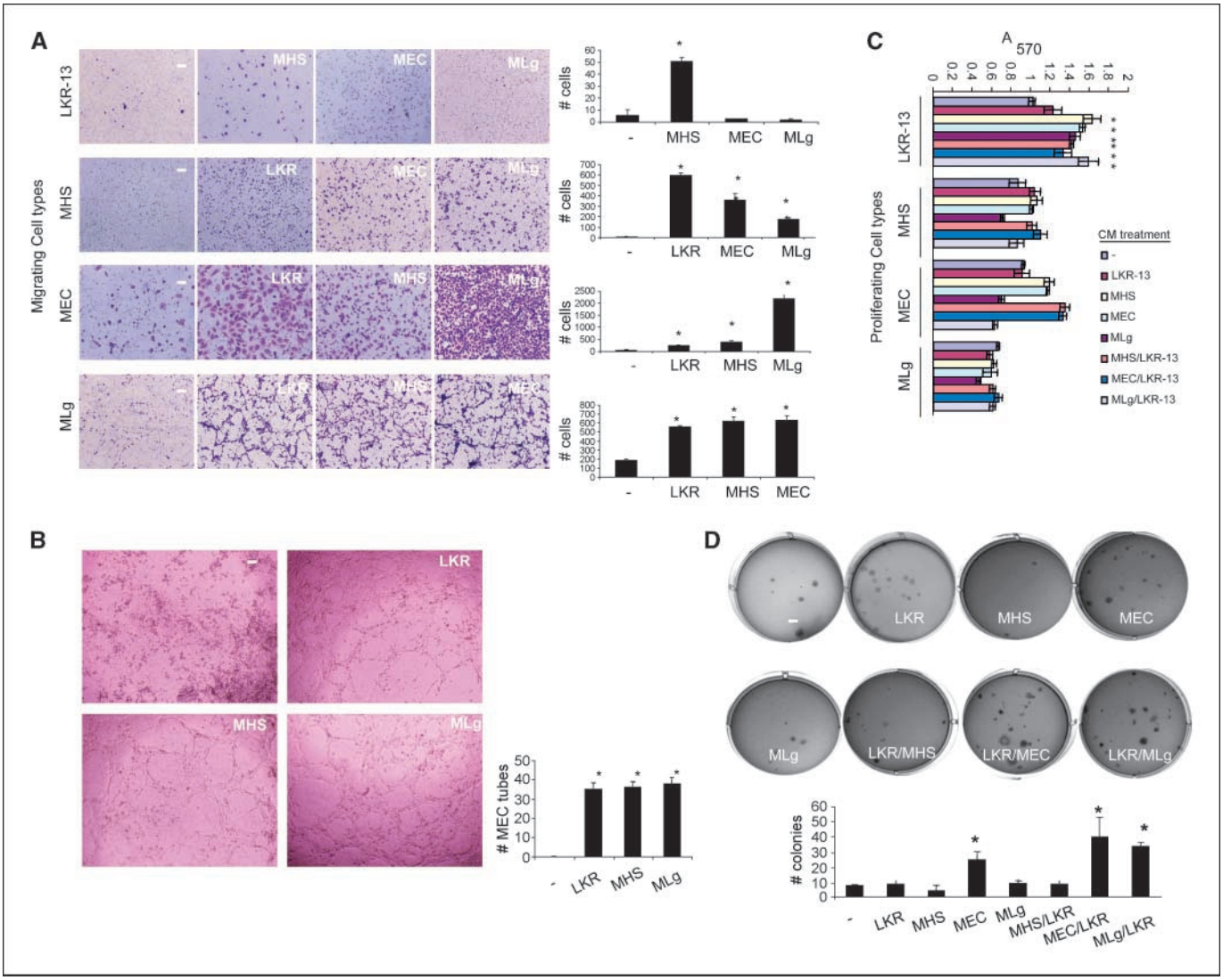

Figure 1. The coculture model. *A* and *B,* cells in the *in vitro* model chemoattract each other and induce MEC tube formation. Cocultures were performed to evaluate cell migration (*A*) and MEC tube formation (*B*). *A,* cells in the top chambers (migrating cell types) were monocultured (–) or cocultured (cell types in the bottom chambers indicated in the top right inset of each picture). Photographs illustrate migrating cells (*A*) and MEC tubes (*B*). Migrating cells and MEC tubes were counted in at least five separate microscopic fields per well, which were averaged, and the mean values per well (±SD) were calculated from replicate wells (bar graphs). *C* and *D,* treatment with conditioned medium samples increases the proliferation of MECs and LKR-13 cells. *C,* cells in monolayer were treated for 24 h with conditioned medium samples and subjected to MTT assays. *D,* LKR-13 cells were seeded in soft agar and treated for 14 d with conditioned medium samples, photographed, and quantified. The cell types (monoculture or coculture) from which the conditioned media samples were collected and used as treatments are indicated (*C,* legend for the MTT assays; *D,* bottom edge of each photographed well). *Columns,* mean values of (*C*) relative cell densities and (*D*) colony numbers were calculated from replicate samples; *bars,* SD. *, $P < 0.05$. *A* and *B,* coculture versus monoculture; *C* and *D,* conditioned medium versus unconditioned medium.

conditioned media samples (data not shown). Thus, IL-18 was sufficient to induce MEC tube formation, and IL-18 inhibition attenuated the ability of LKR-13 cells to chemoattract stromal cells and to proliferate in anchorage-independent conditions.

To genetically inhibit IL-18, LKR-13 cells were transiently transfected with *IL-18* shRNA retroviral vectors. Two different *IL-18* shRNA constructs (A and B) that target different coding sequences were used to evaluate whether they induced consistent biological effects. ELISA of conditioned media samples revealed that IL-18 was inhibited in both transfectants (A and B), and Western blot analysis of nuclear factor-κB (NF-κB), a downstream mediator of IL-18, showed accumulation of NF-κB in the cytoplasm, which is consistent with NF-κB inactivation (Fig. 3*A*). IL-18 depletion from LKR-13 cells inhibited their ability to chemoattract stromal cells in coculture (Fig. 3*B*). We next evaluated whether IL-18 depletion attenuated LKR-13 cell proliferation in monolayer cultures and tumorigenicity in syngeneic (129/SV) mice. For this experiment, we generated LKR-13 cells stably transfected with *IL-18*–specific shRNA (vector A). ELISA of conditioned media samples revealed that IL-18 secretion was inhibited in the *IL-18*–specific shRNA stable transfectants relative to that of control transfectants (Fig. 3*C*). In monolayer cultures, the *IL-18*–depleted LKR-13 cells exhibited reduced proliferation (Fig. 3*C*). Three weeks after s.c. injection in syngeneic mice (n = 4 per group), the *IL-18*–depleted tumors were much smaller than the control tumors (Fig. 3*C*). Thus, IL-18 inhibition attenuated the ability of LKR-13 cells to chemoattract stromal cells, to proliferate in monolayer cultures, and to form tumors in syngeneic mice.

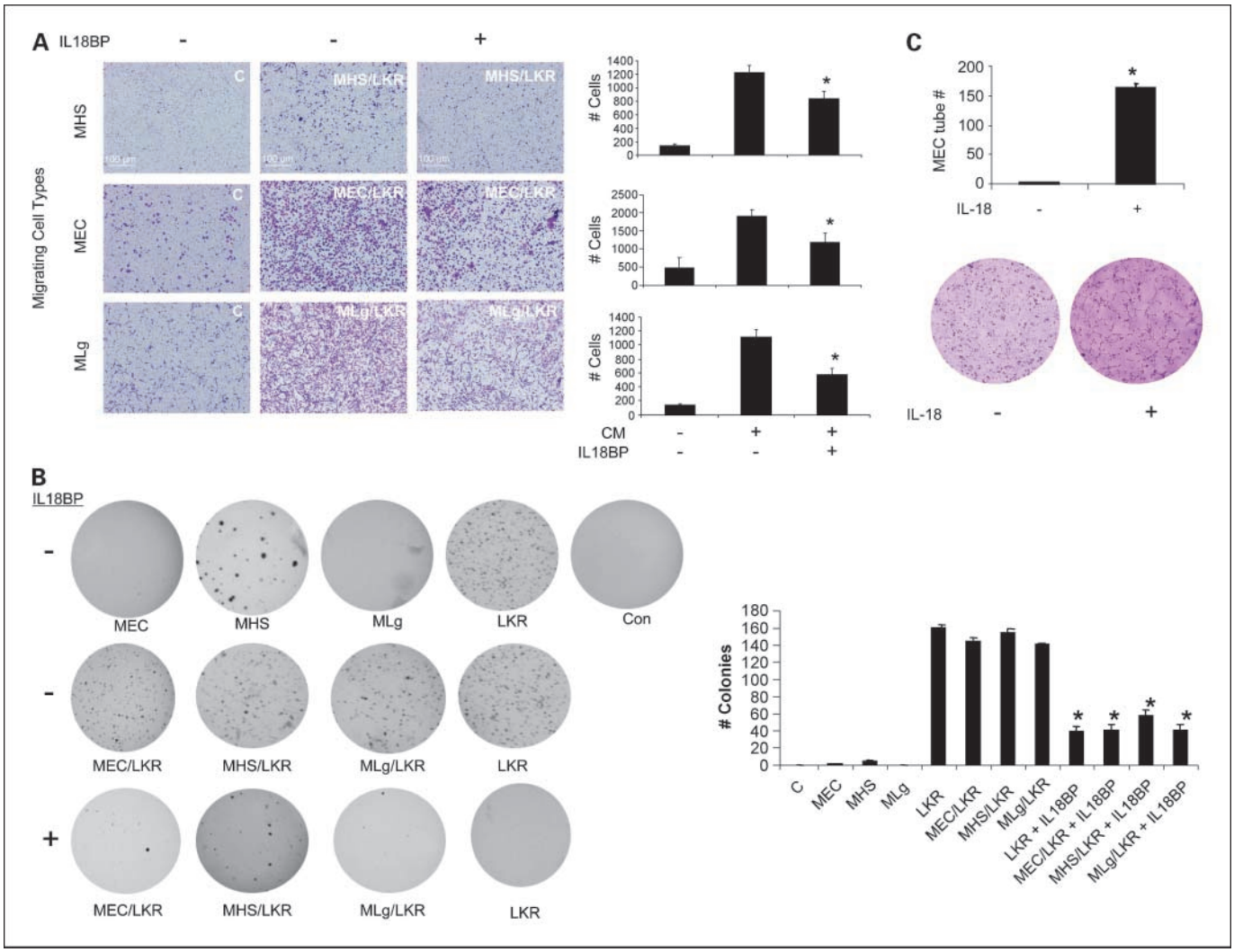

Figure 2. IL-18 promotes bidirectional interactions between LKR-13 cells and stromal cells. *A,* IL-18BP abrogates stromal cell migration induced by conditioned media samples obtained from cocultures. Stromal cells (migrating cell types) were seeded in the top chamber. The bottom chambers were loaded with unconditioned medium (*C*) or conditioned medium samples in the presence (+) or absence (−) of IL-18BP. The cell types (monocuture or coculture) from which the conditioned media samples were collected and used as treatments are indicated at top right inset of each photographed well. Photographs illustrate migrated cells in representative wells. Cells were counted in at least five separate microscopic fields per well, which were averaged, and the mean values per well (±SD) were calculated from replicate wells (adjacent bar graphs). *, $P < 0.05$ (IL-18BP versus no treatment). *B,* IL-18BP abrogates LKR-13 colony formation. LKR-13 cells were seeded in soft agar and treated for 14 d with unconditioned medium (*Con*) or conditioned medium samples in the presence (+) or absence (−) of IL-18BP, photographed, and quantified (bar graphs). *Columns,* mean values of replicate wells; *bars,* SD. The cell types from which the conditioned media samples were collected and used as treatments are indicated underneath each photographed well. *, $P < 0.05$ (IL-18BP versus no treatment). *C,* IL-18 induces MEC tube formation. Photographs illustrate MECs in the presence (+) or absence (−) of recombinant IL-18 (200 ng/well). MEC tubes were counted in at least five separate microscopic fields per well, which were averaged, and the mean values per well (±SD) were calculated from replicate wells (bar graphs). *, $P < 0.05$ (recombinant IL-18 versus no treatment).

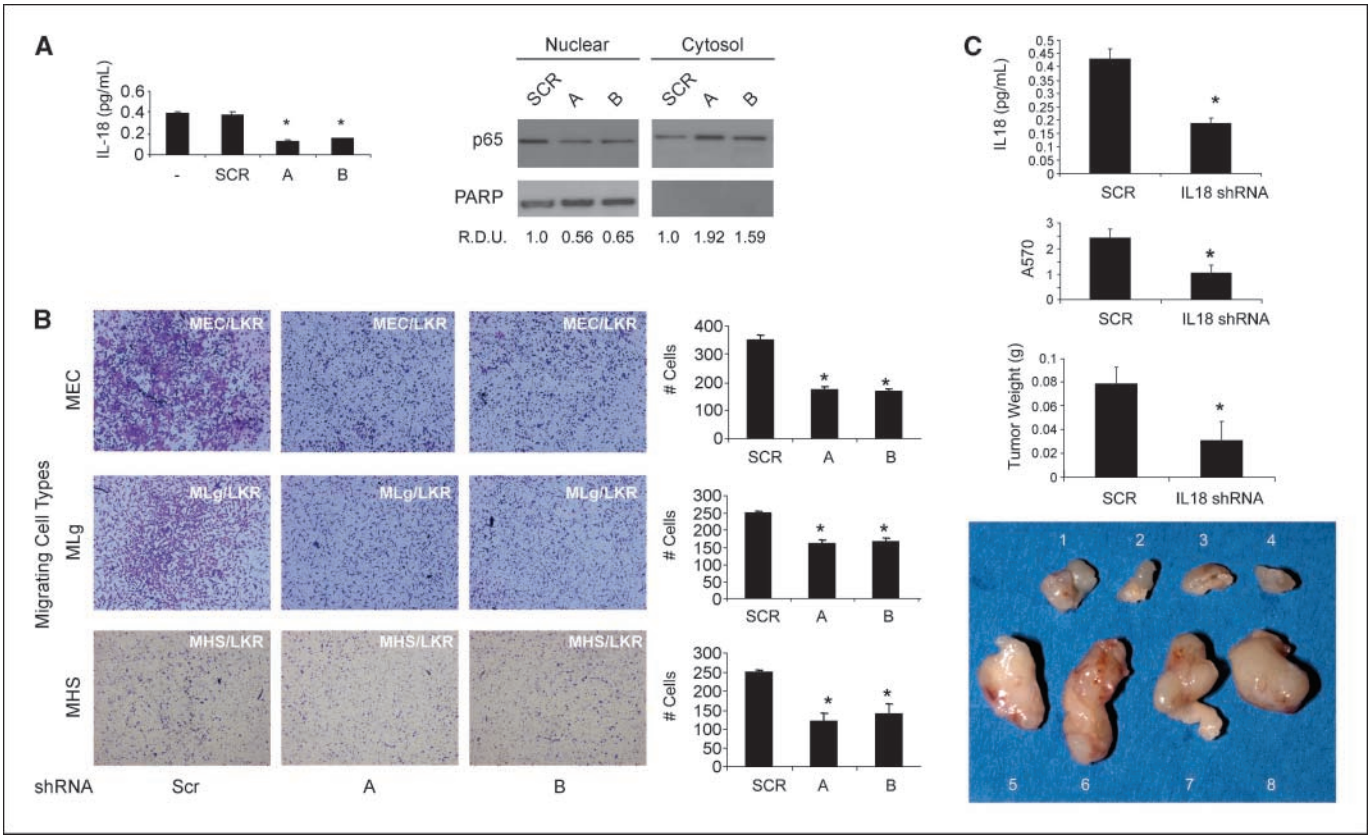

Figure 3. IL-18 promotes bidirectional interactions between LKR-13 cells and stromal cells and enhances LKR-13 cell tumorigenicity. *A,* transfection of *IL-18* shRNA decreases IL-18 secretion and inhibits NF-κB activation in LKR-13 cells. *Left,* IL-18 ELISA of conditioned media samples; *right,* Western blot analysis of p65 in cytoplasmic and nuclear fractions of LKR-13 cells transfected with *IL-18*–specific shRNA vectors (*A* or *B*) or scrambled shRNA control (*Scr*). The expression of poly(ADP-ribose) polymerase (*PARP*) in nuclear but not cytoplasmic fractions on Western blotting indicates fractionation efficiency. Intensities of p65 bands in shRNA transfectants were measured by densitometric scanning and expressed relative to that of scrambled control transfectants (relative densitometric units). *B,* transfection of *IL-18* shRNA inhibits stromal cell migration. Stromal cells (migrating cell types) were seeded in the top chamber, and LKR-13 cells transfected with *IL-18*-specific shRNA vectors (*A* or *B*) or scrambled shRNA control (*Scr*) were seeded into the bottom chamber. Photographs illustrate migrated cells in representative wells. Cells were counted in at least five separate microscopic fields per well, which were averaged, and the mean values per well (±SD) were calculated from replicate wells. *, $P < 0.05$ (scrambled versus *A* or *B*). *C,* IL-18 depletion attenuates LKR-13 cell proliferation and tumorigenicity. *Top bar graph,* IL-18 ELISA performed on conditioned media samples from LKR-13 cells stably transfected with *IL-18*–specific shRNA (vector *A*) or control shRNA; *middle bar graph,* stable LKR-13 transfectants were seeded in monolayer cultures and their density was measured by MTT assays after 72 h in culture. *Columns,* mean values per well calculated from replicate wells; *bars,* SD. *Bottom bar graph and image,* stable LKR-13 transfectants were injected s.c. into syngeneic mice ($n = 4$ per group). Mice were sacrificed after 21 d, and the resulting tumors were removed, photographed (*IL-18*–specific shRNA, tumors 1–4; scrambled controls, tumors 5–8), and weighed (mean ± SD of four tumors in each group).

Discussion

Here, we developed an *in vitro* model to evaluate the mechanisms by which stromal cells regulate the biological properties of lung adenocarcinoma cells. Several lines of evidence suggest that the *in vitro* model recapitulated features of $Kras^{LA1}$ mice and NSCLC patients. First, LKR-13 cells chemoattracted stromal cells, mimicking the intratumoral inflammation and angiogenesis in $Kras^{LA1}$ mice and NSCLC patients (4, 5, 7, 8). Second, conditioned media samples from the cocultures enhanced LKR-13 cell proliferation and clonogenicity, similar to the mitogenic effect of factors secreted into the tumor microenvironment of $Kras^{LA1}$ mice (7, 8). Third, some of the chemokines and cytokines found to be regulated in this *in vitro* model (CCL2, VEGF, CCL5, CXCL1, CXCL2, and CCL11) are also highly expressed in lung tumors in mice and humans (4, 7). Fourth, CXCL1 secretion was enhanced in the cocultures, and CXCR2 inhibition attenuated cell-cell interactions, which is consistent with the observation that CXCR2 ligands promote malignant progression in $Kras^{LA1}$ mice and NSCLC patients (4, 7). We concluded that, because the *in vitro* model recapitulated features of lung tumorigenesis *in vivo*, it might serve as a useful model of the NSCLC tumor microenvironment.

By using two different proteomic approaches, we profiled the secretome of LKR-13 cells and evaluated its regulation by stromal cells. Many of the proteins secreted by LKR-13 cells have been implicated in neoplastic transformation. For example, in cancer cells, tenascin XB, E-cadherin, and biglycan promote cellular adhesion; osteopontin and cathepsin H have been implicated in invasion; clusterin and LIF are prosurvival molecules; CXCL1, CCL3, LIF, IL-18, TNFα, and IL-15 are proinflammatory molecules; and CXCL1, osteopontin, CX3CL1, VEGF, vascular cell adhesion molecule-1, and agrin promote tumor angiogenesis (23–39). Although many of these proteins were secreted basally in monocultures, others (CXCL1, CCL3, VEGF, IL-18, and LIF) were undetectable basally but increased in response to cell-cell interactions. Depletion of IL-18 resulted in attenuation of LKR-13 cell tumorigenicity, indicating that one of the proteins expressed in response to stromal cell interactions was tumorigenic in LKR-13 cells.

An unexpected finding from the proteomic studies was the modulation of biochemical markers of EMT in the cocultures. The cocultures exhibited reduced E-cadherin and loss of cell adhesion and extracellular matrix molecules. Although not definitive evidence of EMT, these changes are closely associated with the loss of cell adhesion and aberrant cell polarity that typify EMT (20). In fact, previous reports support the possibility that cells in the tumor stroma induce neighboring cancer cells to undergo EMT by secreting prostaglandins and cytokines (40, 41). Other findings presented here argue against EMT as a feature of these cocultures. Analysis of their ability to invade through Matrigel revealed that LKR-13 cells did not exhibit enhanced invasive properties when cocultured with stromal cells (data not shown). Furthermore, the abundance of proteases known to promote invasion (osteopontin and cathepsin H) clearly decreased in the cocultures (Table 1). Collectively, these findings suggest that interactions with stromal cells did not induce LKR-13 cells to fully undergo EMT but raise the possibility that stromal cell interactions might facilitate this process.

We found that LKR-13 cells induced MEC tube formation in cocultures. Several lines of evidence suggest that LKR-13 cells induced angiogenesis through a redundant network of cytokines. First, multiple proangiogenic cytokines (VEGF, IL-18, and CXCL1) increased in the cocultures. Second, treatment with recombinant IL-18 was sufficient to induce MEC tube formation. Third, pretreatment of conditioned media samples with neutralizing antibodies against CXCR2 did not abrogate MEC tube formation, indicating that factors within the conditioned media samples could compensate for the loss of a single cytokine. Paradoxically, certain proangiogenic molecules derived from LKR-13 cells (CX3CL1, vascular cell adhesion molecule-1, and agrin) decreased in the cocultures. This may be part of a negative feedback loop activated by stromal cells in response to the proangiogenic mediators of LKR-13 cells, which clearly increased the numbers of endothelial tubes when cocultured with MECs.

Treatment strategies that target the tumor stroma have been implemented in NSCLC patients. For example, bevacisumab, an anti-VEGF neutralizing antibody, enhances tumor shrinkage and prolongs NSCLC patient survival when given in combination with cytotoxic anticancer agents (42, 43). These findings lay the groundwork for clinical trials with agents that target other peptides in the tumor microenvironment. Findings presented here and previously in $Kras^{LA1}$ mice (7) provide a compelling rationale to test the efficacy of inhibitors of CXCL1, IL-18, and possibly other cytokines identified in the coculture model. These inhibitors may be efficacious in patients with *K-ras* mutant NSCLC alone or in combination with VEGF antagonists on the basis of a previous report that CXCR2 ligands drive angiogenesis in tumors that have been rendered VEGF refractory (44).

Disclosure of Potential Conflicts of Interest

No potential conflicts of interest were disclosed.

Acknowledgments

Received 4/23/2008; revised 5/30/2008; accepted 6/4/2008.

Grant support: R01 CA117965 and P50 CA70907.

The costs of publication of this article were defrayed in part by the payment of page charges. This article must therefore be hereby marked *advertisement* in accordance with 18 U.S.C. Section 1734 solely to indicate this fact.

References

1. Sica A, Bronte V. Altered macrophage differentiation and immune dysfunction in tumor development. J Clin Invest 2007;117:1155–66.
2. Mehrad B, Keane MP, Strieter RM. Chemokines as mediators of angiogenesis. Thromb Haemost 2007;97: 755–62.
3. von der Thusen JH, Kuiper J, van Berkel TJ, Biessen EA. Interleukins in atherosclerosis: molecular pathways and therapeutic potential. Pharmacol Rev 2003;55:133–66.
4. Arenberg DA, Keane MP, DiGiovine B, et al. Epithelial-neutrophil activating peptide (ENA-78) is an important angiogenic factor in non-small cell lung cancer. J Clin Invest 1998;102:465–72.
5. Huang M, Wang J, Lee P, et al. Human non-small cell lung cancer cells express a type 2 cytokine pattern. Cancer Res 1995;55:3847–53.
6. Aviel-Ronen S, Blackhall FH, Shepherd FA, Tsao MS. K-ras mutations in non-small-cell lung carcinoma: a review. Clin Lung Cancer 2006;8:30–8.
7. Wislez M, Fujimoto N, Izzo JG, et al. High expression of ligands for chemokine receptor CXCR2 in alveolar epithelial neoplasia induced by oncogenic kras. Cancer Res 2006;66:4198–207.
8. Wislez M, Spencer ML, Izzo JG, et al. Inhibition of mammalian target of rapamycin reverses alveolar epithelial neoplasia induced by oncogenic K-ras. Cancer Res 2005;65:3226–35.
9. Ballin M, Gomez DE, Sinha CC, Thorgeirsson UP. Ras oncogene mediated induction of a 92 kDa metalloproteinase; strong correlation with the malignant phenotype. Biochem Biophys Res Commun 1988;154: 832–8.
10. Okada F, Rak JW, Croix BS, et al. Impact of oncogenes in tumor angiogenesis: mutant K-ras up-regulation of vascular endothelial growth factor/vascular permeability factor is necessary, but not sufficient for tumorigenicity of human colorectal carcinoma cells. Proc Natl Acad Sci U S A 1998;95:3609–14.
11. Sparmann A, Bar-Sagi D. Ras-induced interleukin-8 expression plays a critical role in tumor growth and angiogenesis. Cancer Cell 2004;6:447–58.
12. Watnick RS, Cheng YN, Rangarajan A, Ince TA, Weinberg RA. Ras modulates Myc activity to repress thrombospondin-1 expression and increase tumor angiogenesis. Cancer Cell 2003;3:219–31.
13. Langley RR, Ramirez KM, Tsan RZ, Van Arsdall M, Nilsson MB, Fidler IJ. Tissue-specific microvascular endothelial cell lines from H-2K(b)-tsA58 mice for studies of angiogenesis and metastasis. Cancer Res 2003;63:2971–6.
14. Mbawuike IN, Herscowitz HB. MH-S, a murine alveolar macrophage cell line: morphological, cytochemical, and functional characteristics. J Leukoc Biol 1989; 46:119–27.
15. Yoshikura H, Hirokawa Y. Endogenous C-type virus of a mouse cell line and its defectiveness. J Virol 1974;13: 1319–25.
16. Gronborg M, Kristiansen TZ, Iwahori A, et al. Biomarker discovery from pancreatic cancer secretome using a differential proteomic approach. Mol Cell Proteom 2006;5:157–71.
17. Amanchy R, Kalume DE, Iwahori A, Zhong J, Pandey A. Phosphoproteome analysis of HeLa cells using stable isotope labeling with amino acids in cell culture (SIL-AC). J Proteome Res 2005;4:1661–71.
18. Amanchy R, Kalume DE, Pandey A. Stable isotope labeling with amino acids in cell culture (SIL-AC) for studying dynamics of protein abundance and posttranslational modifications. Sci STKE 2005;2005:pl2.
19. Schulze WX, Mann M. A novel proteomic screen for peptide-protein interactions. J Biol Chem 2004;279: 10756–64.
20. Tse JC, Kalluri R. Mechanisms of metastasis: epithelial-to-mesenchymal transition and contribution of tumor microenvironment. J Cell Biochem 2007;101: 816–29.
21. Park S, Cheon S, Cho D. The dual effects of interleukin-18 in tumor progression. Cell Mol Immunol 2007;4:329–35.
22. Novick D, Kim SH, Fantuzzi G, Reznikov LL, Dinarello CA, Rubinstein M. Interleukin-18 binding protein: a novel modulator of the Th1 cytokine response. Immunity 1999;10:127–36.
23. Chen JJ, Yao PL, Yuan A, et al. Up-regulation of tumor interleukin-8 expression by infiltrating macrophages: its correlation with tumor angiogenesis and patient survival in non-small cell lung cancer. Clin Cancer Res 2003;9:729–37.
24. Batmunkh E, Tatrai P, Szabo E, et al. Comparison of the expression of agrin, a basement membrane heparan sulfate proteoglycan, in cholangiocarcinoma and hepatocellular carcinoma. Hum Pathol 2007;38: 1508–15.
25. Chakraborty G, Jain S, Behera R, et al. The multifaceted roles of osteopontin in cell signaling, tumor progression and angiogenesis. Curr Mol Med 2006;6:819–30.
26. Jedeszko C, Sloane BF. Cysteine cathepsins in human cancer. Biol Chem 2004;385:1017–27.
27. Kim KE, Song H, Kim TS, et al. Interleukin-18 is a critical factor for vascular endothelial growth factor-enhanced migration in human gastric cancer cell lines. Oncogene 2007;26:1468–76.
28. Kurzrock R. The role of cytokines in cancer-related fatigue. Cancer 2001;92:1684–8.
29. Levy P, Ripoche H, Laurendeau I, et al. Microarray-based identification of tenascin C and tenascin XB, genes possibly involved in tumorigenesis associated with neurofibromatosis type 1. Clin Cancer Res 2007;13: 398–407.
30. Mocellin S, Nitti D. TNF and cancer: the two sides of the coin. Front Biosci 2008;13:2774–83.

31. Moretti RM, Marelli MM, Mai S, et al. Clusterin isoforms differentially affect growth and motility of prostate cells: possible implications in prostate tumorigenesis. Cancer Res 2007;67:10325–33.

32. Ren T, Chen Q, Tian Z, Wei H. Down-regulation of surface fractalkine by RNA interference in B16 melanoma reduced tumor growth in mice. Biochem Biophys Res Commun 2007;364:978–84.

33. Saad S, Gottlieb DJ, Bradstock KF, Overall CM, Bendall LJ. Cancer cell-associated fibronectin induces release of matrix metalloproteinase-2 from normal fibroblasts. Cancer Res 2002;62:283–9.

34. Strieter RM, Burdick MD, Mestas J, Gomperts B, Keane MP, Belperio JA. Cancer CXC chemokine networks and tumour angiogenesis. Eur J Cancer 2006;42:768–78.

35. Takenaka Y, Fukumori T, Raz A. Galectin-3 and metastasis. Glycoconj J 2004;19:543–9.

36. Terpos E, Politou M, Viniou N, Rahemtulla A. Significance of macrophage inflammatory protein-1 α (MIP-1α) in multiple myeloma. Leuk Lymphoma 2005; 46:1699–707.

37. Toft DJ, Rosenberg SB, Bergers G, Volpert O, Linzer DI. Reactivation of proliferin gene expression is associated with increased angiogenesis in a cell culture model of fibrosarcoma tumor progression. Proc Natl Acad Sci U S A 2001;98:13055–9.

38. Weber CK, Sommer G, Michl P, et al. Biglycan is overexpressed in pancreatic cancer and induces G_1-arrest in pancreatic cancer cell lines. Gastroenterology 2001;121:657–67.

39. Wu TC. The role of vascular cell adhesion molecule-1 in tumor immune evasion. Cancer Res 2007;67:6003–6.

40. Dohadwala M, Yang SC, Luo J, et al. Cyclooxygenase-2-dependent regulation of E-cadherin: prostaglandin E(2) induces transcriptional repressors ZEB1 and snail in non-small cell lung cancer. Cancer Res 2006;66:5338–45.

41. Xu J, Wang R, Xie ZH, et al. Prostate cancer metastasis: role of the host microenvironment in promoting epithelial to mesenchymal transition and increased bone and adrenal gland metastasis. Prostate 2006;66:1664–73.

42. Sandler A, Gray R, Perry MC, et al. Paclitaxel-carboplatin alone or with bevacizumab for non-small-cell lung cancer. N Engl J Med 2006;355:2542–50.

43. Sandler AB, Gray R, Brahmer J, et al. Randomized phase II/III trial of paclitaxel (P) plus carboplatin (C) with or without bevacizumab (NSC # 04865) in patients with advanced non-squamous non-small cell lung cancer (NSCLC): an Eastern Cooperative Oncology Group (ECOG) trial - E4599. J Clin Oncol 2005;23, No. 16S, Part I of II (June 1 Supplement):4.

44. Mizukami Y, Jo WS, Duerr EM, et al. Induction of interleukin-8 preserves the angiogenic response in HIF-1α-deficient colon cancer cells. Nat Med 2005;11: 992–7.